Conflicts of interest

The authors declare no conflicts of interest.

Highlights

- Tenascin-X (TNX)-deficient mice exhibit significant bone loss

- Osteoclast marker genes are upregulated in TNX-deficient mice

- TNX deficiency promotes osteoclast multinucleation and increased bone resorption

- TNX does not affect osteoblast formation or activity

- Increased osteoclasts resorb bone in TNX deficiency

TNX deficiency results in bone loss due to an increase in multinucleated osteoclasts

Naoyo Kajitani[a, b, *], Takaya Yamada[a], Kohei Kawakami[a] and Ken-ichi Matsumoto[b, *]

[a] Department of Experimental Animals, Interdisciplinary Center for Science Research,

Organization for Research and Academic Information, Shimane University, 89-1 Enya-cho,

Izumo, Shimane 693-8501, Japan

E-mail address:

Naoyo Kajitani: naokaji@med.shimane-u.ac.jp

Takaya Yamada: yamada-t@med.shimane-u.ac.jp

Kohei Kawakami: kkawaka@med.shimane-u.ac.jp

[b] Department of Biosignaling and Radioisotope Experiment, Interdisciplinary Center for

Science Research, Organization for Research and Academic Information, Shimane University,

89-1 Enya-cho, Izumo, Shimane 693-8501, Japan

E-mail address:

Ken-ichi Matsumoto: matumoto@med.shimane-u.ac.jp

* Corresponding author: Ken-ichi Matsumoto (K.-i. Matsumoto)

E-mail address: matumoto@med.shimane-u.ac.jp

Department of Biosignaling and Radioisotope Experiment, Interdisciplinary Center for Science

Research, Organization for Research and Academic Information, Shimane University, 89-1

Enya-cho, Izumo, Shimane 693-8501, Japan. Tel: +81-853-20-2248, Fax: +81-853-20-2248

* Corresponding author: Naoyo Kajitani (N. Kajitani)

E-mail address: naokaji@med.shimane-u.ac.jp

Department of Experimental Animals, Interdisciplinary Center for Science Research,

Organization for Research and Academic Information, Shimane University, 89-1 Enya-cho,

Izumo, Shimane 693-8501, Japan. Tel: +81-853-20-2362, Fax: +81-853-20-2360

Abstract

Tenascin-X (TNX), a glycoprotein of the extracellular matrix (ECM), is expressed in various tissues and plays an important role in ECM architecture. The *TNXB* gene encoding TNX is known as the gene responsible for classic-like Ehlers-Danlos syndrome (clEDS). To date, the role of TNX in dermal, muscular and obstetric features has been reported, but its role in bone homeostasis remains to be clarified. In this study, we found significant bone loss and upregulation of osteoclast marker gene expression in TNX-deficient mice. Further, TNX deficiency in the bone marrow promoted multinucleation of osteoclasts and resulted in increased bone resorption activity. These results indicate that multinucleated osteoclasts are the cause of bone loss in a TNX-deficient environment. Our findings provide new insight into the mechanism of osteoclast differentiation mediated by TNX and the pathology of clEDS.

Keywords

Abbreviations

TNX: Tenascin-X

ECM: extracellular matrix

clEDS: classic-like Ehlers-Danlos syndrome

BMD: bone mineral density

BMMs: bone marrow macrophages

1. Introduction

Extracellular matrix (ECM) plays an important role in regulating various cell behaviours

such as proliferation, differentiation and migration by transducing signals through cell surface

proteins which adhere to the ECM [1-3]. The ECM is an integral player that not only provides

physical support to the cells, but also a dynamic structure which controls tissue homeostasis [4].

Furthermore, the ECM is part of a dynamic environment called a *niche* [5]. Bone tissue consists

mainly of ECM, which in bone is formed of osteoid, an organic matrix composed of type I

collagen, proteoglycans, and hydroxyapatite [6].

Tenascin-X (TNX) which is an ECM glycoprotein encoded by the *TNXB* gene, is the

largest member in the tenascin family [7]. *TNXB* is known to be one of the genes responsible for

Ehlers-Danlos syndrome (EDS), a heritable disorder of connective tissue. The clinical

manifestations of EDS are categorised into 13 subtypes that are characterised by fragility of

skin, blood vessels, internal organs, hypermobility of joints, and other complications [8]. A

small insertion/deletion or a large deletion of the *TNXB* gene is known to be associated with

classical-like Ehlers-Danlos syndrome (clEDS) [9,10]. Symptoms of skin hyperextensibility,

joint hypermobility, easy bruising without atrophic scarring, joint dislocations and chronic pain

are observed in patients with clEDS. Further, osteoporosis is also observed in a subset of

patients with EDS [11-14]. These reports imply that TNX is a possible contributor to bone

homeostasis, but any association is yet to be uncovered.

Mouse TNX has a structure characteristic of tenascin family members, which consists of a signal peptide and four heptad repeats followed by 18.5 epidermal growth factor-like (EGF) repeats, 31 fibronectin type III-like (FNIII) repeats, and a region homologous to fibrinogen [15]. *Tnxb*-KO mice have been found to exhibit characteristic skin, mild muscular and obstetric features, similar to those in EDS patients [16-19]. Thus, *Tnxb*-KO mice are regarded as a model animal for EDS and have been studied to elucidate the mechanism of clEDS pathology.

In the present study, we investigated the bone phenotype and the osteoblastic and osteoclastic differentiation potentials of bone marrow cells in *Tnxb*-KO mice. A balance of osteoblast and osteoclast activities maintains bone homeostasis. Generally, an imbalance between osteoblast and /or osteoclast activities causes low bone mineral density (BMD), bone loss and mechanical strength [20,21]. We show that TNX deficiency enhances osteoclast maturation and activates bone resorption. Our data provide a new insight into the pathology of clEDS in patients with TNX deficiency.

2. Materials and methods

2.1. Mice

Animal experiments were approved by the Ethical Committee for Animal Research of

Shimane University. Wild-type (WT) C57BL6J mice were purchased from CLEA Japan (Tokyo,

Japan) and *Tnxb*-KO mice backcrossed onto C57BL6/J were generated as described previously

[22]. All procedures were performed according to the animal care guidelines of the committee.

2.2. Histological analysis

Bone samples were fixed in 10% formalin, then sent to Kureha Special Laboratory Co.,

Ltd. (Fukushima, Japan), where they were immersed in 10–30% sucrose and embedded in 4%

carboxymethyl cellulose (CMC), then sectioned (5 μm) and stained with hematoxylin and eosin

(HE).

2.3. Analysis of micro-computed tomography (micro-CT)

The dissected femurs were fixed in 10% formalin for 3 days and stored in 70% ethanol.

Then the femurs were wrapped in parafilm and scanned using a Skyscan 1174 microCT

machine (Bruker microCT, Kontich, Belgium) with an X-ray energy of 50 kV and 0.5 mm

aluminium filter. Scanned three-dimensional (3D) images were reconstructed using the NRecon

program (Skyscan). Trabecular bone analysis was performed on the spongiosa region, beginning

1.286 mm below the growth plate and extending 0.643 mm towards the epiphysis of the femur.

Cortical bone analysis was performed on the mid shaft, beginning 3.215 mm below the growth

plate and extending 0.643 mm towards the epiphysis. 3D analysis of trabecular and cortical

bone was performed using the CTAn program (Skyscan). 3D images were generated in CTvol

program (Skyscan).

2.4. Osteoblast and osteoclast differentiation

Primary bone marrow cells were isolated from femurs as described previously [23].

Isolated cells were treated with lysis buffer (BD PharmLyse Buffer; BD Biosciences, Franklin

Lakes, NJ, USA) to eliminate the erythrocytes and washed twice with PBS. The cells were then

seeded into a 24-well plate at 3.5×10^6 cells per well and cultured in α-minimum essential

medium (α-MEM) (Thermo Fisher Scientific, Waltham, MA, USA) containing 10% foetal

bovine serum (FBS) (Thermo Fisher Scientific), and 2 mM GlutaMAX (Thermo Fisher

Scientific). After 4 days, the cells were changed into osteoblast differentiation medium [α-

MEM, 10% FBS, 2 mM L-glutamine, 0.1 μM dexamethasone (Sigma-Aldrich, MO, USA), with

10 mM β-glycerophosphate (Nacalai Tesque, Kyoto, Japan), and 0.3 mM L-ascorbic acid

(Fujifilm Wako Pure Chemical Corporation, Osaka, Japan)] and cultured for 2 weeks.

Afterwards, the cells were fixed with 10% formalin and stained using a calcified nodule staining

kit with alizarin red S (Cosmo Bio Co., Ltd., Tokyo, Japan). For the measurement of calcium

mineralization, 5% formic acid was added and the absorbance of eluted dye at 415 nm was

measured using an Emax precision microplate reader (Molecular Devices, Sunnyvale, CA, USA).

Isolated primary bone marrow cells were seeded into a 24-well plate at 1.5×10^6 cells per well and cultured in α-MEM containing 10% FBS, 2 mM GlutaMAX and 50 ng/mL macrophage colony-stimulating factor (M-CSF) (Fujifilm Wako Pure Chemical Corporation). After 3 days, adherent cells, i.e., bone marrow macrophages (BMMs) were used as osteoclast progenitor cells. BMMs were cultured in osteoclast differentiation medium containing M-CSF and receptor activator of nuclear factor kappa-B ligand (RANKL) (Cosmo Bio Co., Ltd.) for 4 days. The cells were fixed and stained using a tartrate-resistant acid phosphatase (TRAP) staining kit (Fujifilm Wako Pure Chemical Corporation). TRAP-positive multinucleated cells (more than four nuclei) were counted.

2.5. Bone resorption activity assay

BMMs were cultured and osteoclast differentiation was induced on Osteo Assay Plates (Corning Inc., Corning, NY, USA). After the medium was removed, 100 μL of bleach solution (10% kitchen bleach) (Daiichisekken Co., Ltd., Gunma, Japan) was added and incubated for 5 min at room temperature. The wells were washed twice with distilled water and dried at room temperature for 3 to 5 hours. The bone pits generated by osteoclasts were observed using a

microscope (BZ-X710) (Keyence Co., Osaka, Japan), and analysed using image J software

(https://imagej.nih.gov/ij/).

2.6. Reverse transcription (RT), RT-PCR and real-time PCR

Total RNA from crushed bones and cultured cells was extracted using ISOGEN (Nippon

Gene Co., Ltd., Tokyo, Japan) and treated with a Turbo DNA-free kit (Thermo Fisher Scientific)

according to the manufacture's procedure. RT was performed with the PrimeScript 1st strand

cDNA synthesis kit and PrimeScript RT reagent kit (TaKaRa, Shiga, Japan). Synthesized

cDNAs were subjected to RT-PCR using Ex-Taq DNA polymerase (TaKaRa) and to real-time

PCR using SYBR Premix EXTaq II (TaKaRa). All reactions in real-time PCR were performed

in triplicate and the expression of *Hprt* was used for normalization. The primer sequences are

listed in Table 1.

3. Results

3.1. *Tnxb*-KO mice exhibit lower bone mass

To investigate the involvement of TNX deficiency in bone mass, we analysed bone in

Tnxb-KO mice. HE staining indicated that both trabecular bone mass and cortical bone

thickness were reduced in *Tnxb*-KO mice compared with WT mice (Fig. 1A and B). Further,

micro-CT analysis revealed that both the bone mass and BMD of trabecular bone were

significantly lower in *Tnxb*-KO mice than those of age-matched WT mice (Fig. 1C-H). Notably,

the differences were most significant at 10 weeks of age. Meanwhile in the analysis of cortical

bone, BMD, cortical section and medullary area were mostly comparable, but bone volume,

bone area and thickness were markedly lower than in WT mice at 8 months of age (Fig. 1I-O).

These results indicate that TNX contributes particularly to the development of trabecular bone.

3.2. Osteoblast differentiation is not affected by TNX deficiency

Next, we examined whether bone loss in TNX-deficient mice resulted from changes in

osteoblast differentiation. Expression of *Tnxb* mRNA at day 10 of osteoblastic differentiation

was analysed by RT-PCR (Fig. 2A). Osteoblast differentiation ability and calcium

mineralization in bone marrow cells from *Tnxb*-KO mice were comparable to those in WT mice

(Fig. 2B and C).

3.3. Osteoclast differentiation and function are enhanced in *Tnxb*-KO BMMs

To examine the effects of TNX deficiency on osteoclast differentiation, BMMs from WT

and *Tnxb*-KO mice were induced to differentiate into osteoclasts. Fig. 3A shows that the

numbers of TRAP-positive osteoclasts were significantly increased in *Tnxb*-KO BMMs

compared with WT. Interestingly, the number of multinucleated osteoclasts was markedly

increased compared with WT (2.9 ± 2.1 cells in WT BMMs vs 18.9 ± 7.4 cells in *Tnxb*-KO

BMMs) (Fig. 3B). These data were supported by increases in the expression of osteoclast

markers: nuclear factor of activated T cells cytoplasmic 1 (*Nfatc1*), cathepsin K (*Ctsk*), dendritic

cell-specific transmembrane protein (*Dcstamp*) and matrix metalloproteinase-9 (*Mmp9*), were

all higher in *Tnxb*-KO cells during osteoclastic differentiation (Fig. 3C-F). In addition to

osteoclast differentiation, the bone resorbing ability of *Tnxb*-KO osteoclasts was also

significantly higher than in WT cells (Fig. 3G and 3H).

3.4. Expression of bone-associated factors in the bone of *Tnxb*-KO mice

Finally, to examine whether TNX deficiency alters the expression levels of bone-

associated genes *in vivo* as well as *in vitro*, the expression of osteoblast and osteoclast marker

genes was examined. However, no significant differences were observed in osteoblast or

osteoclast markers of WT and *Tnxb*-KO mice (Fig. 4).

4. **Discussion**

Tnxb-KO mice have been studied as model mice for clEDS to elucidate the pathogenic

mechanism of clEDS and the molecular function of TNX. Several reports indicated that *Tnxb*-

KO mice have aberrant phenotypes in skin, muscle, uterus, and blood vessel formation in peripheral nerves [17-19,24,25]. In the present study, we show that *Tnxb*-KO mice had low femoral bone mass (Fig. 1). Furthermore, increased formation of multinucleated osteoclasts and increases in their bone-resorbing ability were observed in *Tnxb*-KO BMMs, although calcium mineralization following osteogenic differentiation was unchanged (Fig. 2 and 3). These results suggest that TNX contributes to the maintenance of bone mass by regulating osteoclast maturation.

Osteoclasts differentiate from BMMs on or near the bone surface[26]. Osteoclast differentiation is induced by activation of receptor activator of nuclear factor kappa-B (RANK) which is expressed on BMMs, and triggers the recruitment of TNF receptor-associated factor (TRAF) family proteins such as TRAF6, followed by activation of downstream signalling pathways such as extracellular signal-regulated kinase (ERK), p38, nuclear factor kappa-B (NF-κB), c-Jun N-terminal kinases (JNK) and c-Fos [26-28]. The activation of these signal pathways upregulates the expression of NFATc1 and its downstream targets such as TRAP, Ctsk, MMP9 and DC-STAMP [29-31]. Notably, DC-STAMP is reported to be an important regulator of osteoclast and macrophage cell fusion, and *DC-STAMP*^{-/-} osteoclasts exhibited abrogated multinucleation [32]. According to our data, the expression of *Dcstamp* in *Tnxb*-KO osteoclasts was higher than in WT osteoclasts, and multinucleated osteoclasts were also increased (Fig. 3).

These suggest that TNX contributes to bone mass by suppressing the multinucleation of osteoclasts.

An adherent environment is also essential for osteoclastogenesis. Miyamoto *et al*. reported that the recognition of arginine-glycine-aspartic acid (RGD) tripeptide-containing ECM proteins by $\alpha_V\beta_3$ integrins in osteoclast precursors is important for osteoclastogenesis [33]. However, no RGD tripeptide was found in mouse TNX although RGD sequences are present in human and bovine [34,35], and hence, the increased number of multinucleated osteoclasts observed in *Tnxb*-KO mice may be an indirect effect exerted via defects of other ECM proteins caused by TNX deficiency. Alternatively, it is possible that there is another unknown peptide recognized as a ligand for the $\alpha_V\beta_3$ integrins in mouse TNX. As another possibility, TNX is secreted by fibroblasts and the serum form of TNX (sTNX) is detected in mice [36,37], therefore the secreted form of TNX produced by osteoblasts and/or other cells may contribute to the regulation of osteoclast differentiation via its interaction with $\alpha_V\beta_3$ integrins on the surface of osteoclast precursor cells. In support of this theory, *Tnxb* expression was detected during osteoblast differentiation but not osteoclast differentiation (Fig. 2A and data not shown).

Finally, no significant differences in the expression of osteoblast or osteoclast markers were observed in bone from *Tnxb*-KO and WT mice, but markers did show a tendency to be higher in *Tnxb*-KO mice (Fig. 4). In particular, DC-STAMP plays a critical role in cell–cell

14

fusion in osteoclasts and macrophages [38]. This is in agreement with our findings in which

TNX deficiency promoted the multinucleation of osteoclasts (Fig. 3). Therefore, these data

suggest that bone loss in *Tnxb*-KO mice is likely to be caused by the increase in the number of

multinucleated osteoclasts.

In summary, we investigated defects of bone metabolism in TNX-deficient mice and our

results indicated significant bone loss. In addition, our data indicated that TNX-deficient BMMs

facilitated multinucleation of osteoclasts during osteoclast differentiation. Our work provides a

new understanding of clEDS pathology, but further investigation is needed to clarify the

molecular mechanism of bone metabolism in TNX deficiency.

References

[1] D.E. Discher, D.J. Mooney, P.W. Zandstra, Growth factors, matrices, and forces combine and control stem cells, Science 324 (2009) 1673-1677. 10.1126/science.1171643.

[2] A.L. Berrier, K.M. Yamada, Cell-matrix adhesion, J Cell Physiol 213 (2007) 565-573. 10.1002/jcp.21237.

[3] R.O. Hynes, The extracellular matrix: not just pretty fibrils, Science 326 (2009) 1216-1219. 10.1126/science.1176009.

[4] C. Bonnans, J. Chou, Z. Werb, Remodelling the extracellular matrix in development and disease, Nat Rev Mol Cell Biol 15 (2014) 786-801. 10.1038/nrm3904.

[5] F. Gattazzo, A. Urciuolo, P. Bonaldo, Extracellular matrix: a dynamic microenvironment for stem cell niche, Biochim Biophys Acta 1840 (2014) 2506-2519. 10.1016/j.bbagen.2014.01.010.

[6] F. Taraballi, G. Bauza, P. McCulloch, J. Harris, E. Tasciotti, Concise Review: Biomimetic Functionalization of Biomaterials to Stimulate the Endogenous Healing Process of Cartilage and Bone Tissue, Stem Cells Transl Med 6 (2017) 2186-2196. 10.1002/sctm.17-0181.

[7] R.P. Tucker, K. Drabikowski, J.F. Hess, J. Ferralli, R. Chiquet-Ehrismann, J.C. Adams, Phylogenetic analysis of the tenascin gene family: evidence of origin early in the chordate lineage, BMC Evol Biol 6 (2006) 60. 10.1186/1471-2148-6-60.

[8] F. Malfait, Vascular aspects of the Ehlers-Danlos Syndromes, Matrix Biol 71-72 (2018) 380-395.

10.1016/j.matbio.2018.04.013.

[9] J. Schalkwijk, M.C. Zweers, P.M. Steijlen, W.B. Dean, G. Taylor, I.M. van Vlijmen, B. van Haren,

W.L. Miller, J. Bristow, A recessive form of the Ehlers-Danlos syndrome caused by tenascin-X deficiency,

N Engl J Med 345 (2001) 1167-1175. 10.1056/NEJMoa002939.

[10] M.C. Zweers, J. Bristow, P.M. Steijlen, W.B. Dean, B.C. Hamel, M. Otero, M. Kucharekova, J.B.

Boezeman, J. Schalkwijk, Haploinsufficiency of TNXB is associated with hypermobility type of Ehlers-

Danlos syndrome, Am J Hum Genet 73 (2003) 214-217. 10.1086/376564.

[11] A.A. Deodhar, A.D. Woolf, Ehlers Danlos syndrome and osteoporosis, Ann Rheum Dis 53 (1994)

841-842.

[12] L. Carbone, F.A. Tylavsky, A.J. Bush, W. Koo, E. Orwoll, S. Cheng, Bone density in Ehlers-Danlos

syndrome, Osteoporos Int 11 (2000) 388-392. 10.1007/s001980070104.

[13] J.L. Yen, S.P. Lin, M.R. Chen, D.M. Niu, Clinical features of Ehlers-Danlos syndrome, J Formos

Med Assoc 105 (2006) 475-480. 10.1016/S0929-6646(09)60187-X.

[14] S.J. Theodorou, D.J. Theodorou, Y. Kakitsubata, J.E. Adams, Low bone mass in Ehlers-Danlos

syndrome, Intern Med 51 (2012) 3225-3226.

[15] T. Ikuta, N. Sogawa, H. Ariga, T. Ikemura, K. Matsumoto, Structural analysis of mouse tenascin-X:

evolutionary aspects of reduplication of FNIII repeats in the tenascin gene family, Gene 217 (1998) 1-13.

[16] T. Minamitani, T. Ikuta, Y. Saito, G. Takebe, M. Sato, H. Sawa, T. Nishimura, F. Nakamura, K.

Takahashi, H. Ariga, K. Matsumoto, Modulation of collagen fibrillogenesis by tenascin-X and type VI

collagen, Exp Cell Res 298 (2004) 305-315. 10.1016/j.yexcr.2004.04.030.

[17] D.F. Egging, I. van Vlijmen, B. Starcher, Y. Gijsen, M.C. Zweers, L. Blankevoort, J. Bristow, J.

Schalkwijk, Dermal connective tissue development in mice: an essential role for tenascin-X, Cell Tissue

Res 323 (2006) 465-474. 10.1007/s00441-005-0100-5.

[18] N.C. Voermans, K. Verrijp, L. Eshuis, M.C. Balemans, D. Egging, E. Sterrenburg, I.A. van Rooij,

J.A. van der Laak, J. Schalkwijk, S.M. van der Maarel, M. Lammens, B.G. van Engelen, Mild muscular

features in tenascin-X knockout mice, a model of Ehlers-danlos syndrome, Connect Tissue Res 52 (2011)

422-432. 10.3109/03008207.2010.551616.

[19] D.F. Egging, I. van Vlijmen-Willems, J. Choi, A.C. Peeters, D. van Rens, G. Veit, M. Koch, E.C.

Davis, J. Schalkwijk, Analysis of obstetric complications and uterine connective tissue in tenascin-X-

deficient humans and mice, Cell Tissue Res 332 (2008) 523-532. 10.1007/s00441-008-0591-y.

[20] M. Zaidi, Skeletal remodeling in health and disease, Nat Med 13 (2007) 791-801. 10.1038/nm1593.

[21] R. Aggarwal, J. Lu, S. Kanji, M. Joseph, M. Das, G.J. Noble, B.K. McMichael, S. Agarwal, R.T.

Hart, Z. Sun, B.S. Lee, T.J. Rosol, R. Jackson, H.Q. Mao, V.J. Pompili, H. Das, Human umbilical cord

blood-derived CD34+ cells reverse osteoporosis in NOD/SCID mice by altering osteoblastic and

osteoclastic activities, PLoS One 7 (2012) e39365. 10.1371/journal.pone.0039365.

[22] K. Hashimoto, N. Kajitani, Y. Miyamoto, K.I. Matsumoto, Wound healing-related properties detected

in an experimental model with a collagen gel contraction assay are affected in the absence of tenascin-X, Exp Cell Res 363 (2018) 102-113. 10.1016/j.yexcr.2017.12.025.

[23] D.D. Houlihan, Y. Mabuchi, S. Morikawa, K. Niibe, D. Araki, S. Suzuki, H. Okano, Y. Matsuzaki, Isolation of mouse mesenchymal stem cells on the basis of expression of Sca-1 and PDGFR-alpha, Nature Protocols 7 (2012) 2103-2111. 10.1038/nprot.2012.125.

[24] H. Sakai, S. Yokota, N. Kajitani, T. Yoneyama, K. Kawakami, Y. Yasui, K.I. Matsumoto, A potential contribution of tenascin-X to blood vessel formation in peripheral nerves, Neurosci Res 124 (2017) 1-7. 10.1016/j.neures.2017.06.003.

[25] R. Aktar, M. Peiris, A. Fikree, V. Cibert-Goton, M. Walmsley, I.R. Tough, P. Watanabe, E.J.A. Araujo, S.D. Mohammed, J.M. Delalande, D.C. Bulmer, S.M. Scott, H.M. Cox, N.C. Voermans, Q. Aziz, L.A. Blackshaw, The extracellular matrix glycoprotein tenascin-X regulates peripheral sensory and motor neurones, J Physiol 596 (2018) 4237-4251. 10.1113/JP276300.

[26] W.J. Boyle, W.S. Simonet, D.L. Lacey, Osteoclast differentiation and activation, Nature 423 (2003) 337-342. 10.1038/nature01658.

[27] H. Hsu, D.L. Lacey, C.R. Dunstan, I. Solovyev, A. Colombero, E. Timms, H.L. Tan, G. Elliott, M.J. Kelley, I. Sarosi, L. Wang, X.Z. Xia, R. Elliott, L. Chiu, T. Black, S. Scully, C. Capparelli, S. Morony, G. Shimamoto, M.B. Bass, W.J. Boyle, Tumor necrosis factor receptor family member RANK mediates osteoclast differentiation and activation induced by osteoprotegerin ligand, Proc Natl Acad Sci U S A 96

(1999) 3540-3545.

[28] K. Matsuo, J.M. Owens, M. Tonko, C. Elliott, T.J. Chambers, E.F. Wagner, Fosl1 is a transcriptional target of c-Fos during osteoclast differentiation, Nat Genet 24 (2000) 184-187. 10.1038/72855.

[29] M. Asagiri, K. Sato, T. Usami, S. Ochi, H. Nishina, H. Yoshida, I. Morita, E.F. Wagner, T.W. Mak, E. Serfling, H. Takayanagi, Autoamplification of NFATc1 expression determines its essential role in bone homeostasis, J Exp Med 202 (2005) 1261-1269. 10.1084/jem.20051150.

[30] M. Asagiri, H. Takayanagi, The molecular understanding of osteoclast differentiation, Bone 40 (2007) 251-264. 10.1016/j.bone.2006.09.023.

[31] Y. Miyauchi, K. Ninomiya, H. Miyamoto, A. Sakamoto, R. Iwasaki, H. Hoshi, K. Miyamoto, W. Hao, S. Yoshida, H. Morioka, K. Chiba, S. Kato, T. Tokuhisa, M. Saitou, Y. Toyama, T. Suda, T. Miyamoto, The Blimp1-Bcl6 axis is critical to regulate osteoclast differentiation and bone homeostasis, J Exp Med 207 (2010) 751-762. 10.1084/jem.20091957.

[32] M. Yagi, T. Miyamoto, Y. Sawatani, K. Iwamoto, N. Hosogane, N. Fujita, K. Morita, K. Ninomiya, T. Suzuki, K. Miyamoto, Y. Oike, M. Takeya, Y. Toyama, T. Suda, DC-STAMP is essential for cell-cell fusion in osteoclasts and foreign body giant cells, J Exp Med 202 (2005) 345-351. 10.1084/jem.20050645.

[33] T. Miyamoto, F. Arai, O. Ohneda, K. Takagi, D.M. Anderson, T. Suda, An adherent condition is required for formation of multinuclear osteoclasts in the presence of macrophage colony-stimulating

factor and receptor activator of nuclear factor kappa B ligand, Blood 96 (2000) 4335-4343.

[34] F. Elefteriou, J.Y. Exposito, R. Garrone, C. Lethias, Cell adhesion to tenascin-X mapping of cell

adhesion sites and identification of integrin receptors, Eur J Biochem 263 (1999) 840-848.

[35] U. Valcourt, L.B. Alcaraz, J.Y. Exposito, C. Lethias, L. Bartholin, Tenascin-X: beyond the

architectural function, Cell Adh Migr 9 (2015) 154-165. 10.4161/19336918.2014.994893.

[36] T. Sakai, Y. Furukawa, R. Chiquet-Ehrismann, M. Nakamura, S. Kitagawa, T. Ikemura, K.

Matsumoto, Tenascin-X expression in tumor cells and fibroblasts: glucocorticoids as negative regulators

in fibroblasts, J Cell Sci 109 (Pt 8) (1996) 2069-2077.

[37] K. Matsumoto, T. Kinoshita, T. Hirose, H. Ariga, Characterization of mouse serum tenascin-X, DNA

Cell Biol 25 (2006) 448-456. 10.1089/dna.2006.25.448.

[38] M. Yagi, T. Miyamoto, Y. Toyama, T. Suda, Role of DC-STAMP in cellular fusion of osteoclasts and

macrophage giant cells, J Bone Miner Metab 24 (2006) 355-358. 10.1007/s00774-006-0697-9.

Figure legends

Figure 1. *Tnxb*-KO mice exhibit lower bone mass.

(A and B) HE staining of representative sections of the distal femur and femoral diaphysis from 10-week-old WT mice and *Tnxb*-KO mice (n = 3), scale bars, 500 μm. (C) Representative 3D reconstructions of trabecular bone from 4-week-old, 10-week-old and 8-month-old WT and *Tnxb*-KO mice, scale bars, 500 μm. (D-H) Quantitative changes in trabecular bone parameters by micro-CT. (D) Trabecular bone mineral density (trabecular BMD; g/cm^3), (E) trabecular percent bone volume (bone volume per total volume; BV/TV; %), (F) trabecular thickness (Tb.Th; μm), (G) trabecular separation (Tb.Sp; μm) and (H) trabecular number (Tb.N; mm^{-1}). (I) Representative 3D reconstructions of cortical bone from 4-week old, 10-week old and 8-month old WT and *Tnxb*-KO mice, scale bars, 500 μm. (J-O) Quantitative changes in cortical bone parameters by micro-CT. (J) Cortical bone mineral density (cortical BMD; g/cm^3), (K) cortical percent bone volume (bone volume per total volume; BT/TV; %), (L) cortical section area (T.Ar; mm^2), (M) cortical bone area (B.Ar; mm^2), (N) medullary area (T.Ar-B.Ar; mm^2) and (O) cortical thickness (Ct.Th.; mm). Data are presented as means ± SE, n = 5, $*P < 0.05$; $**P < 0.005$ by *t*-test.

Figure 2. Osteoblast differentiation is not affected by TNX-deficiency.

(A) Expression of *Tnxb* mRNA in osteogenic differentiation. Primary bone marrow cells were isolated from 7-week old WT mice. Actin (*Actb*) mRNA was used as an internal control. (B) Alizarin red staining of osteogenic differentiation. Data are representative of five experiments. (C) Measurement of calcium mineralization. The absorbance of eluted dye from alizarin red-stained cells was measured at 415 nm. Data are presented as means ± SE of five experiments.

Figure 3. Osteoclast differentiation and function are enhanced in *Tnxb*-KO BMMs.

(A) TRAP staining of differentiated osteoclasts from WT and *Tnxb*-KO BMMs. (B) Number of TRAP-positive multinucleated cells (> 4 nuclei). Data are means ± SE of 6 wells from two experiments. $**P < 0.005$ by *t*-test. Scale bars, 200 μm. (C–F) Relative expression of osteoclast marker genes, (C) *Nfatc1*, (D) *Dcstamp*, (E) *Ctsk* and (E) *Mmp9* at indicated time-points during osteoclastogenesis. Data are presented as means ± SE of three experiments. $*P < 0.05$, $**P < 0.005$ by *t*-test. (G) Osteoclasts were removed from the Osteo Assay Plate and photographed. (H) The resorption pit areas were analysed using image J. Data are means ± SE of 9 wells from two experiments. $**P < 0.005$ by *t*-test. Sale bars, 200 μm. Data are representative of two experiments.

Figure 4. Expression of bone-associated factors in bone of *Tnxb*-KO mice.

23

(A) Expression of *Tnxb* mRNA in bone from 10-week-old WT and *Tnxb*-KO mice, analysed by

RT-PCR. *Actb* mRNA was used as the internal control. (B–F) Expression of osteoblast marker

genes, (B) *Runx2*, (C) *Alp*, and osteoclast marker genes, (D) *Nfatc1*, (E) *Dcstamp*, (F) *Ctsk*.
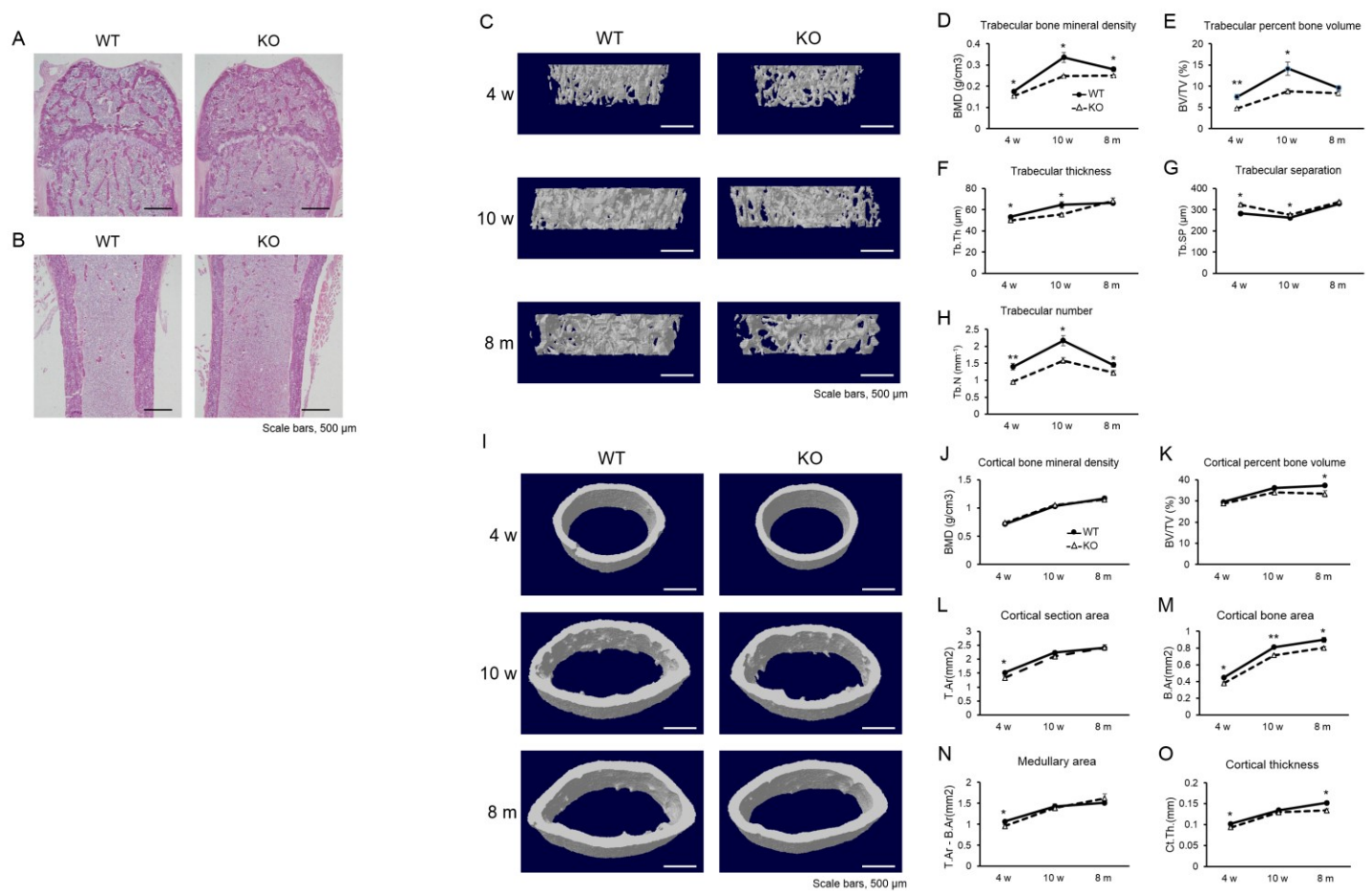
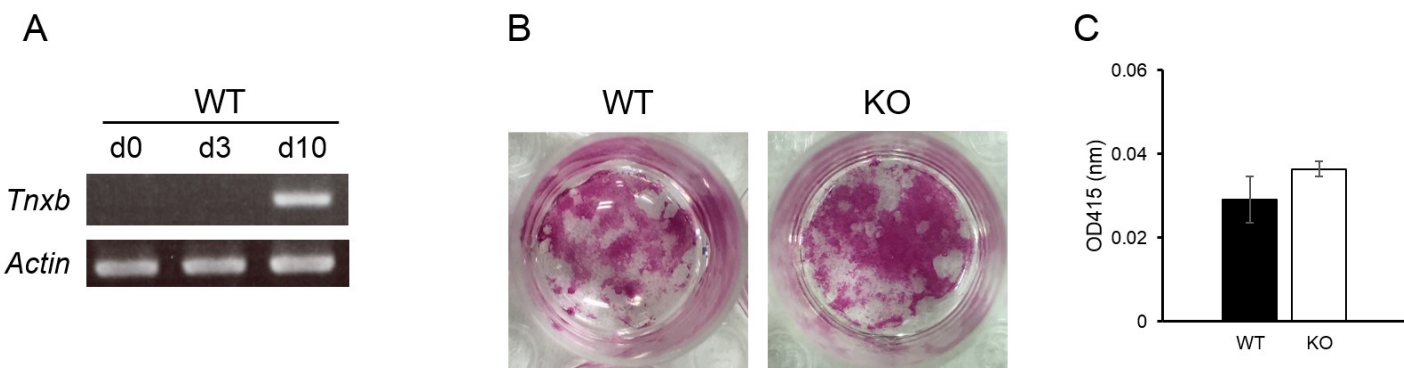Data are presented as means ± SE of three individual mice.

Figure 1. Kajitani *et al*.

A

WT

	d0	d3	d10
Tnxb			
Actin			

B

WT   KO

C

OD415 (nm)

Figure 2. Kajitani *et al*.

A

WT   KO

Scale bars, 500 μm

B

C   *Nfatc1*

D   *Dcstamp*

E   *Ctsk*

F   *Mmp9*

G

WT   KO

Scale bars, 200 μm

H

Figure 3. Kajitani *et al*.

A RT-PCR
WT   KO

Tnxb

Actin

B *Runx2*

Relative mRNA expression (WT, KO)

C *Alp*

Relative mRNA expression (WT, KO)

D *Nfatc1*

Relative mRNA expression (WT, KO)

E *Dcstamp*

Relative mRNA expression (WT, KO)

F *Ctsk*

Relative mRNA expression (WT, KO)

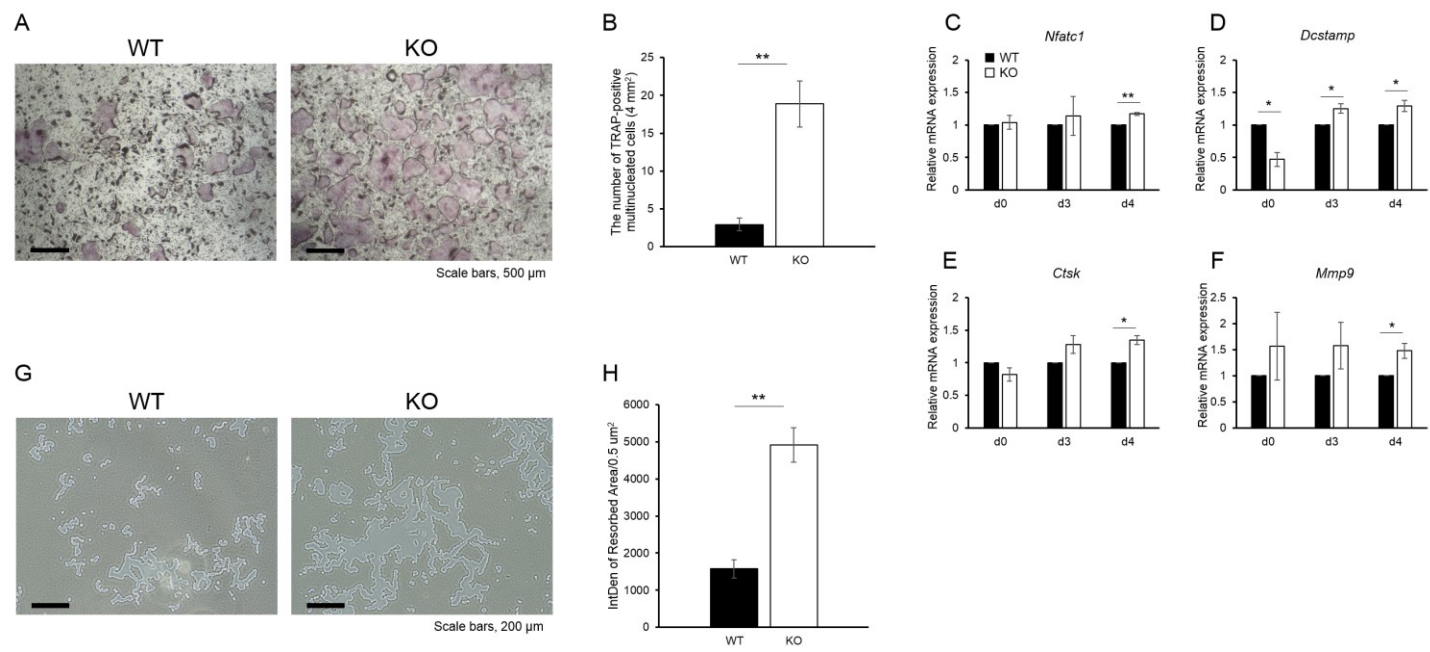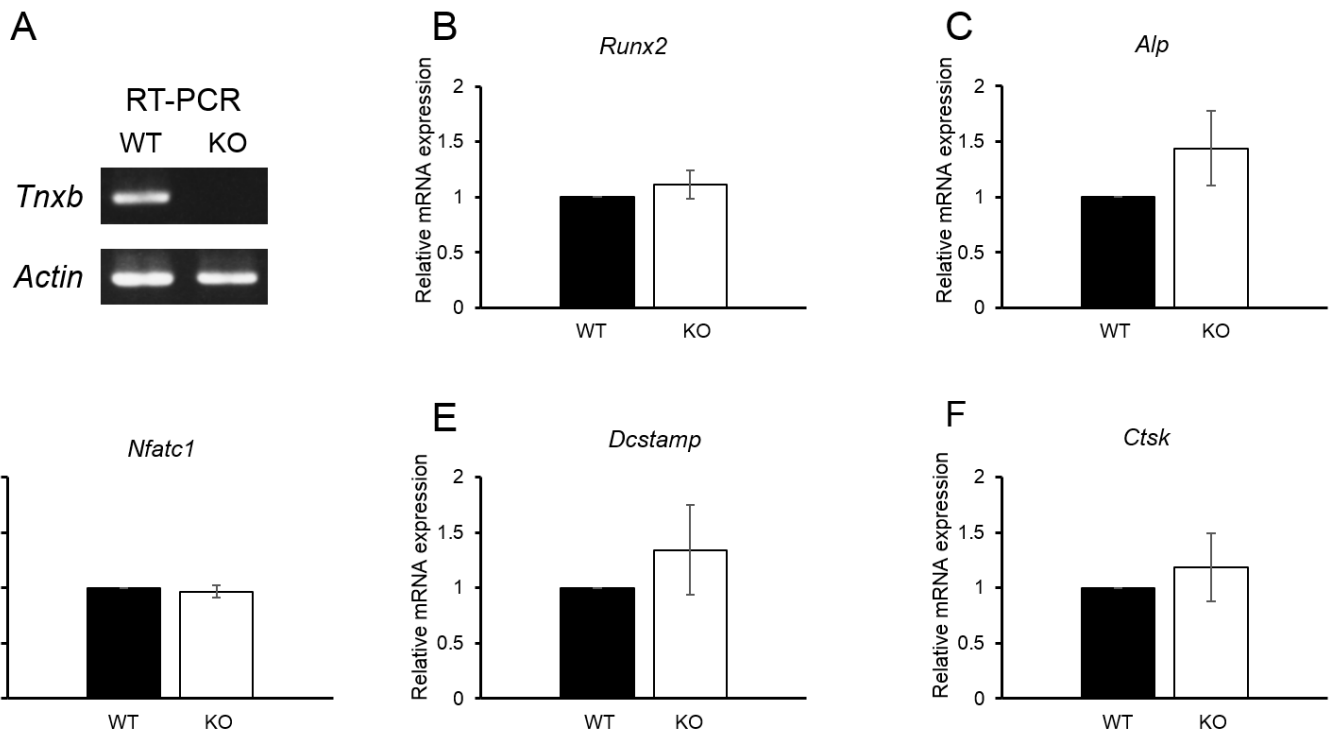Figure 4. Kajitani *et al*.

Table 1. Primer sequences used for Real-time PCR and RT-PCR analysis.

For real-time PCR

Target gene		Sequence (5'-3')	Amplified product
Hprt	Fwd	TCCTCCTCAGACCGCTTTT	90 bp
	Rev	CCTGGTTCATCATCGCTAATC	
Alp	Fwd	CGGATCCTGACCAAAAACC	74 bp
	Rev	TCATGATGTCCGTGGTCAAT	
Runx2	Fwd	GCCCAGGCGTATTTCAGA	82 bp
	Rev	TGCCTGGCTCTTCTTACTGAG	
Ctsk	Fwd	CGAAAAGAGCCTAGCGAACA	67 bp
	Rev	TGGGTAGCAGCAGAAACTTG	
Dcstamp	Fwd	CGAAGCTCCTTGAGAAACGA	96 bp
	Rev	GGACTGGAAACCAGAAATGAA	
Nfatc1	Fwd	GGTAACTCTGTCTTTCTAACCTTAAGCTC	240 bp
	Rev	GTGATGACCCCAGCATGCACCAGTCACAG	
Tnxb	Fwd	TCCTGGAGGAGCTGGTAAAA	127 bp
	Rev	AGGTCAAAGACACCGTGGAG	
Mmp9	Fwd	GCGGACATTGTCATCCAGTTTG	130 bp
	Rev	CGTCGTCGAAATGGGCATC	

For RT-PCR

Tnxb	Fwd	ATGGCAGCTCAGTGCACCCCGTCTA	413 bp
	Rev	AAGACACCGTGGAGGCTGCAGAGGC	
Actb	Fwd	TACCACGGGCATTGTGATGG	546 bp
	Rev	GATCTTGATCTTCATGGTGC	